Polymer Chemistry

Accepted Manuscript

This is an *Accepted Manuscript*, which has been through the Royal Society of Chemistry peer review process and has been accepted for publication.

Accepted Manuscripts are published online shortly after acceptance, before technical editing, formatting and proof reading. Using this free service, authors can make their results available to the community, in citable form, before we publish the edited article. We will replace this *Accepted Manuscript* with the edited and formatted *Advance Article* as soon as it is available.

You can find more information about *Accepted Manuscripts* in the Information for Authors.

Please note that technical editing may introduce minor changes to the text and/or graphics, which may alter content. The journal's standard Terms & Conditions and the Ethical guidelines still apply. In no event shall the Royal Society of Chemistry be held responsible for any errors or omissions in this *Accepted Manuscript* or any consequences arising from the use of any information it contains.

ROYAL SOCIETY OF CHEMISTRY

www.rsc.org/polymers

Tuning Oxygen Permeability in Azobenzene-Containing Side-Chain Liquid Crystalline Polymers

Author(s), and Corresponding Authors:

*Syed Hassan, Robinson Anandakathir, Margaret J. Sobkowicz and Bridgette M. Budhlall**

Department of Plastics Engineering and NSF Center for High-Rate Nanomanufacturing, University of Massachusetts, Lowell, MA. 01854.

*Corresponding author email: Bridgette_Budhlall@uml.edu

†Electronic supplementary information (ESI) available: Experimental details, characterization data and additional figures.

Keywords: liquid crystalline polymers, odd-even effect, responsive polymer, permeability

Abstract

A series of poly[4-(4-cyanoazobenzene-4'-oxy)alkyl methacrylate]s, side-chain liquid crystalline polymers (azoLCP) were synthesized with methylene groups as spacers varying from 5 to 12. The thermal properties and phase transition temperatures of the polymers were characterized with differential scanning calorimetry and polarized optical microscopy and a relationship between spacer lengths, glass transition (T_g) and clearing temperatures (T_c) of the polymers was established. The T_g decreased with increasing spacer length, while the T_c exibited an odd-even effect with varying spacer length. X-ray diffraction was used to determine the degree crystallinity above and below T_c. The azoLCPs exhibited smectic ↔ nematic ↔ isotropic phases. Increasing crystallinity correlated linearly with decreasing gas permeability as

measured using an oxygen permeation analyzer, which was used to measure the films' permeability to oxygen (O_2) gas. Switching of the azoLCPs from a liquid crystalline to an isotropic state was accomplished by heating the films above their T_c, which resulted in at least a 10-fold increase in the O_2 permeability coefficient (P_{O_2}). Increasing the methylene spacer length of the azoLCP had little or no effect on gas permeability however it did decrease the T_c, allowing fine control of the temperature at which the switch in P_{O_2} takes place by tuning the mesophase between nematic and isotropic states.

Introduction

Liquid crystalline polymers (LCPs) are considered to be promising smart polymers which exhibit mesomorphism meaning that they can change their phases and properties in response to temperature, pH, infrared or ultraviolet (UV) light.[1,2] Because of their unique properties, LCPs have been used for several applications including artificial muscle actuators, highly selective membranes and optoelectronic devices.[3,4,5,6] Side-chain liquid crystalline polymers (SCLCP) are unique polymer structures in which the polymer backbone is connected to a stimuli-responsive moiety by methylene spacer group.

The spacer length between the main chain and mesogen also plays an important role in liquid crystalline properties of the polymer, where nematic order has been observed in SCLCP with short spacers and smectic order was observed with long spacers.[1] SCLCPs show a decrease in glass transition temperature (T_g) and clearing temperature[2] (T_c) as the number of methylene spacer groups increases.[7,8] This effect is associated with plasticization of backbone by the side chain.[7] Decrease in T_g and T_c also stems from increased distance between mesogens and the backbone that results in lower steric hindrance.[9]

Changes in X-ray diffraction intensities have been used to distinguish between mesomorphic behaviors of liquid crystalline polymers. Intensities and location of diffraction peaks are used to measure inter-layer packing and lamellar spacing orders in SCLCPs.[10] Incorporation of azobenzene mesogens into polymers leads to liquid crystalline behavior. Several studies have revealed that photoisomerization of azobenzene molecules can change orientation of molecules from crystalline domains to randomly ordered isotropic domains which can in turn change the permeability behavior of the polymer.[11]

Recently, Liu *et al.* demonstrated the controlled gas permeability through SCLCP with an azobenzene mesogen when the orientation of the mesogen is switched using non-polarized and circularly polarized light.[4] This research found that the crystalline phase of the SCLCP is least susceptible to permeating molecules as compared to permeability in isotropic phase. These findings are an important step towards attaining reversible photo-induced switchability; but they lack in providing further discussion on changing permeability behavior with changing SCLCP structure i.e. the effect of length of the spacer group. A remaining ambiguity in that work is the separation of the cooperative effects of annealing and photo-switching using circularly polarized light; which failed to clearly explain the differences in mesophase behavior. In summary, Liu's research failed to shed light on the role of mesophase structure and the resultant change in permeability response in their SCLCP.

Kajiyama *et al.* reported on a series of liquid crystalline membrane systems and their ability to tune permeability when incorporated in polyvinyl chloride and polycarbonate host materials.[12] These polymer systems showed enhanced analyte permeability and selectivity in hydrocarbon separation through while switching between crystalline-nematic-isotropic phase transitions. Recently, Marshal *et al.* reported that liquid crystalline moieties embedded in polymers have been used in switchable membranes for nitrogen.[11] The liquid crystalline material used as an active element in the membranes required energy equivalent to 2 mW/cm^2 for 5 seconds to switch from nematic to isotropic phase. They also studied the effect of azobenzene dopant concentration on reversible permeability characteristics of liquid crystalline (LC) materials. Even though they showed reversible permeability behavior they were unable to resolve the conflict between liquid crystalline mesophases and photoswitchable permeability.

Permeability was not only a function of reversible phase switching of LC materials but also the pore sizes of the membrane in which the LC material was embedded.

It was originally hypothesized here that the permeability of SCLCPs can be tuned by changing the length of the spacer group due to the changing distance between the polymer backbone and azobenzene moiety. Therefore, the motivation for using SCLCP is the ability to tune the orientational and positional ordering of the crystalline domains by varying the spacer length. The design of the SCLCP consists of a poly(methacrylate) backbone with an azobenzene moiety given the acronym azoLCP-C$_n$, where n represents the number of methylene groups in the spacer connecting the azobenzene mesogen as depicted in **Fig. 1**.

It was found however, as will be described in this article, that increasing the methylene spacer length had little or no effect on O_2 gas permeability (P_{O_2}), instead it did decrease the T_c, allowing fine control of the temperature at which the switch in P_{O_2} takes place by tuning the mesophase between nematic and an isotropic state.

The motivation for using poly(methacrylate) is the ease of synthesis via free radical polymerization, noted flexibility and strength of poly(methacrylate) films and the ability to tune the minimum film formation temperature by controlling the polymer T_g thus being able to achieve free-standing polymer films and coatings at ambient-use temperatures.

Herein, the synthesis and structure-property relationships of selectively permeable azobenzene-containing to SCLCP films that could be used to control the timing of exposure of gas vapors to its environment are described. Free-standing SCLCP films that can be used control the timing of gas permeability have been developed. The permeability of the films was increased in a controlled manner by exposure to an external stimulus (heat). It is proposed that these films

could be used in selectively permeable coatings which respond to external stimuli to control gas permeability. For example, these thermally responsive azoLCP films can be applied to textiles to achieve "*smart*" textile functionality whereby the gas vapor permeability increases at higher temperatures (to promote cooling) and decreases at lower temperatures (to trap warm air) thereby protecting the wearer from dramatic temperature changes in the environment.

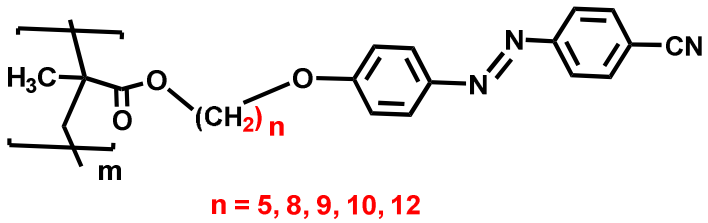

Fig. 1 Chemical structure of azobenzene containing side-chain liquid crystalline polymer (azoLCP-C$_n$): Poly(*n*-[4-(4'-cyanophenylazo)phenoxy]alkyl$_n$ methacrylate with varying methylene spacer groups, *n*.

Results and Discussion

The relationship between switchable gas permeability properties and LC mesophase structures of a series of azoLCPs was studied by characterizing the chemical structure using nuclear magnetic resonance (NMR), Fourier transform infra-red (FTIR) spectroscopy and gel permeation chromatography (GPC); the thermal properties by thermo-gravimetric analysis (TGA), and differential scanning calorimetry (DSC); and mesomorphic phase behavior by polarizing optical microscopy (POM) which was confirmed by X-ray diffraction (WAXD).

Finally, we analyzed oxygen permeability through azoLCP films using permeability analysis with oxygen (O_2) gas.

Synthesis of a Homologous Series of azoLCPs and Characterization of their Microstructure

Poly(*n*-[4-(4'-cyanophenylazo)phenoxy]alkyl$_n$ methacrylate) (azoLCP-C$_n$) where the spacer chain length, *n* was varied such that *n* = 5 or 8, 9, 10 or 12, was synthesized using the general proceedure described previously[13] and shown schematically in **Fig. 2**. The structures of the intermediates, monomers and polymers were characterized with ^{1}H NMR, FTIR and UV-Vis spectroscopy. The NMR spectra for each monomer step and each of the respective poly[*n* (4'-cyanophenylazo)phenoxy] methacrylate azopolymers (azoLCP-C_5, C_8 C_9, C_{10} and C_{12}) are shown in the Electronic Supporting Information (ESI†).

The aromatic protons of monomer **4** were found at δ7.98 ppm, 7.77 and δ7.00 ppm which were similar to the precursor bromo compound **3**. The vinyl hydrogens of the methacrylate group appeared at δ6.07 and 5.52 ppm. The NMR signals disappeared completely after polymerization, confirming that the monomer underwent polymerization, producing azoLCPs. The azoLCPs are readily soluble in common organic solvents such as THF, chloroform and acetone.

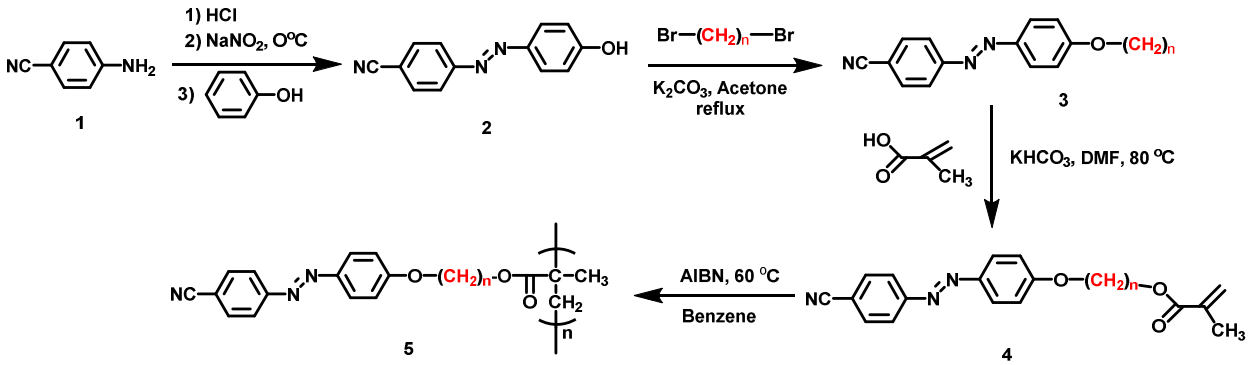

Fig. 2 Synthesis of Poly(*n*-[4-(4'-cyanophenylazo)phenoxy]alkyl methacrylate) where the methylene spacer chain length, *n* was varied such that *n* = 5, 8, 9, 10 or 12.

Molecular Weight Analysis using GPC

For the series of poly[4-(4'-cyanophenylazo)phenoxy]alkyl methacrylate polymers (azoLCP-C$_n$) the weight average molecular weight (M_w) and number average molecular weight (M_n) and was in the range 4,640 to 6,290 g/mol and 3,280 to 5,360 g/mol respectively, as shown for each polymer in **Table 1**. The polydispersity index (PDI) ranged from ~1.14 to ~1.55. These M_n corresponded to average degrees of polymerization (*DP*) ranging from 9-14, which are statistically not significantly different.

These relatively low molecular weights are typical for azobenzene containing polymers synthesized by free-radical polymerization.[14] It is speculated that there is an inhibition of the azobenzene moieties to free-radical polymerization, resulting in low-efficiency of monomer conversion and low polymer molecular weights.[15] It has been reported that when AIBN (10 wt%) was used as an initiator, the polymerization of 40-((2-(acryloyloxy)ethyl)ethylamino)-4-nitroazobenzene required 96 hrs to achieve 4,000 g/mol molecular weight polymer.[16,17]

Table 1 Molecular weights, polydispersity index (PDI) and number average degrees of polymerization (*DP*) for the azoLCP-C_n series

AzoLCP (spacer)	*Yield (%)*	M_w *(g/mol)*	M_n *(g/mol)*	*PDI*	*DP*
azoLCP-(CH_2)5	76	5,640	3,740	1.50	10
azoLCP-(CH_2)8	54	6,290	5,360	1.17	14
azoLCP-(CH_2)9	70	5,570	4,850	1.14	13
azoLCP-(CH_2)10	60	5,440	4,000	1.36	11
azoLCP-(CH_2)12	45	4,640	3,280	1.55	9

Thermal Phase Behavior using TGA and DSC

TGA was first used to measure thermal stability of the polymers as shown in **Fig. 3**. From the TGA data, it can be seen that the polymer is thermally stable up to 300 ^{o}C. As seen in the plots in **Fig. 3**, the polymer had three mass loss events centered around 350 °C, 450 °C and 575 °C corresponding to degradation of different parts of the polymer structure. It is hypothesized that there is potential unzipping due to reactive chain ends[18] in the polymer around 350-375 °C, breaking up of CH_2 spacer groups occurring around 450 ^{o}C, and finally the benzene rings decomposing at higher temperature event, with little or no char remaining. The degradation temperature at the onset of 5 wt% mass loss, $T_{(5\% \text{ onset loss})}$ for the series of azoLCPs is shown in **Table 2**. It was observed that $T_{(5\% \text{ onset loss})}$ decreased slightly with increasing spacer length, as larger methylene spacer groups start to decompose at lower enthalpic values.

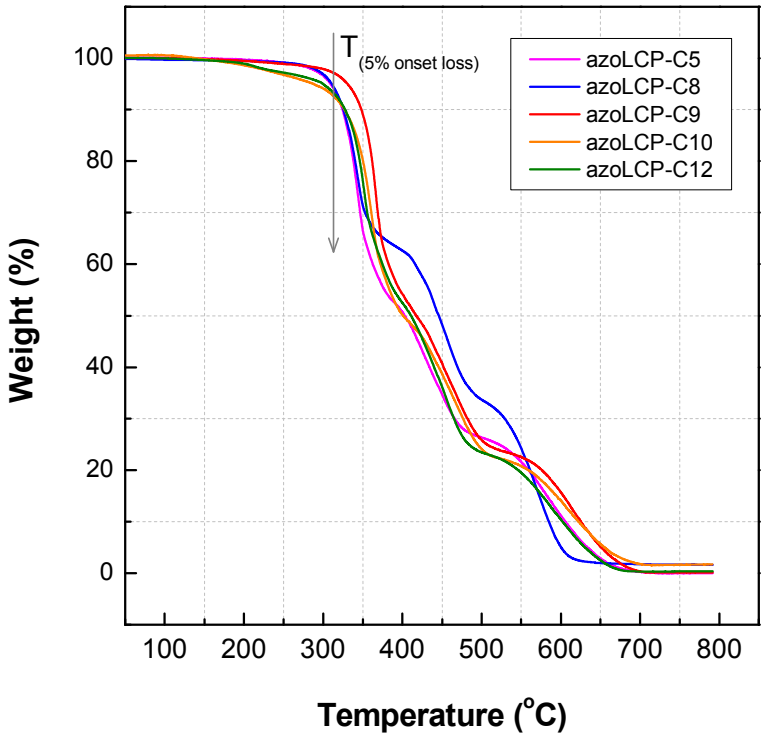

Fig. 3 Thermal gravimetric analysis of poly[4-(4'-cyanophenylazo)phenoxy]alkyl methacrylate polymers (azoLCP-C_5, C_8, C_9 C_{10} and C_{12}) measured at a heating rate of 15°C/min.

DSC was used to determine the phase transition temperatures of the series of azoLCPs synthesized with varying spacer lengths**.** From the initial DSC heating cycle, all azoLCPs show a first-order endothermic peak associated with a smectic to nematic (T_{SN}) transition (ESI **Fig. S8-12†**). The second heating cycle is shown in **Fig. 4**, where another endothermic peak attributed to the nematic to isotropic (T_{NI}) or clearing transition (T_c) and a second-order transition indicative of the glass transition (T_g) temperature were observed. The area under the endotherms in the initial and second heating DSC scans used to determine the corresponding entropies $\Delta S_{SN}/R$ and

the $\Delta S_{NI}/R$ for the smectic and nematic phases respectively are shown in **Table 2**, where R is the universal gas constant (8.314462 J mol^{-1} K^{-1}).

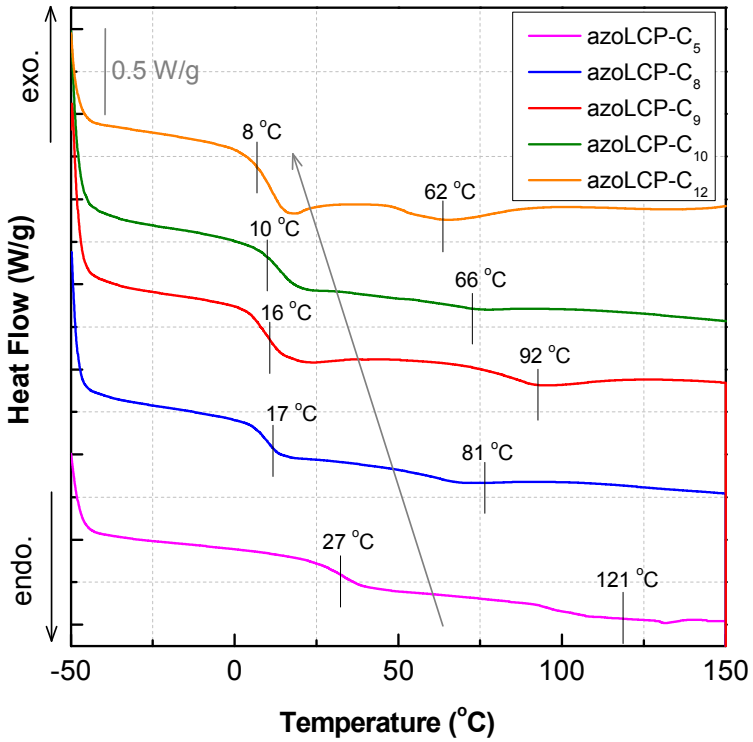

Fig. 4 DSC thermographs of poly[4-(4'-cyanophenylazo)phenoxy]alkyl methacrylate polymers (azoLCP-C_5, C_8, C_9 C_{10} and C_{12}) indicating T_g and T_c during the second heating cycle. The plots are offset for clarity of presentation. The arrow indicates increasing methylene spacer length.

Table 2 Thermal and mesomorphic properties for poly[4-(4'-cyanophenylazo)phenoxy]alkyl methacrylate polymers (azoLCP-C_5, C_8, C_9, C_{10} and C_{12}) extracted from the second heating cycle in the DSC thermographs unless noted otherwise

AzoLCP (spacer)	$T_{(5\%\ onset)}$ (°C) *	T_g (°C)	T_{SN} ‡ (°C)	T_{NI} (°C)	ΔH_{SN} (kJ mol^{-1})	ΔS_{SN} ‡ (kJ K^{-1} mol^{-1})	$\Delta S_{SN}/R$ ‡	ΔH_{NI} (kJ mol^{-1})	ΔS_{NI} (kJ K^{-1} mol^{-1})	$\Delta S_{NI}/R$
azoLCP-(CH_2)5	344	27	44	121	0.10	0.31	0.04	0.26	2.15	0.26
azoLCP-(CH_2)8	312	17	-	81	-	-	-	1.03	12.75	1.53
azoLCP-(CH_2)9	331	16	48	92	0.20	0.62	0.07	1.69	18.46	2.22
azoLCP-(CH_2)10	290	10	42-51	66	0.80	2.48	0.30	0.51	7.64	0.92
azoLCP-(CH_2)12	300	8	14	62	1.33	4.63	0.56	2.08	33.58	4.04

* Temperatures obtained from TGA at the onset of 5% weight loss.

‡ Temperatures obtained from the initial heat cycle in the DSC thermographs.

As shown in **Table 2**, is a decreasing trend is evident in the T_g and T_{NI} temperatures with increasing methylene spacer length. In fact, the azoLCP-C$_n$ followed the thermal behavior of a similar homologous series of poly[(4-cyanoazobenzene-4'-oxy)alkyl methacrylate]s also studied by Imrie *et al*. (1998),[13] where a decrease in T_g and T_{NI} temperatures with increasing methylene spacer length was observed as shown in **Table 2** and **Fig. 5**. This decreasing trend in T_g is not unique to cyanoazobenzene mesogens, as a similar trend was observed for SCLCPs with polymethacrylates based on *p*-methoxyazobenzene.[19] For a homologous series of SCLCPs composed of the same polymer and similar molecular weight, the decrease in T_g with increasing spacer length is explained by a plasticization effect of flexible spacer groups on the polymer backbone[13,20] or the increasing decoupling of the side chains from the backbone polymer.[20,21]

In addition, there is an odd-even effect in clearing temperature, T_c or nematic to isotropic temperature, T_{NI} in the series of azoLCP-C$_n$ as shown in **Fig. 5**, similar to that reported by Imrie *et al*. (1998)[13] for SCLCPs bearing azobenzene mesogens with a cyano tail group. It is observed that the spacer groups with odd-numbers of C atoms give higher T_c than those with even-numbers. It is speculated that for an odd-numbered spacer group the orientation of the mesogen group lies orthogonal to the polymer backbone compared to the even-numbered spacer group, where the mesogen is thought to align at an angle with regard to the polymer backbone. Such orientation of the mesogens in the latter case results in less anisotropic interactions between the mesogens and therefore reduced clearing or isotropic temperatures.[13]

The dependence of the entropy associated with the smectic-nematic ($\Delta S_{SN}/R$) and nematic-isotropic (clearing) ($\Delta S_{NI}/R$) transitions as a function of varying spacer length, *n* for the azoLCPs is shown in **Table 2** and **Fig. 6**. Both entropies increased with increasing methylene

spacer length, with $\Delta S_{NI}/R$ exhibiting an odd-even effect similar to that reported by Imrie *et al*. (1998)[13] and (1995)[7] for SCLCPs bearing azobenzene and cyanobiphenyl mesogens with a cyano tail group, respectively. Indeed, the odd-even effect shown by both the clearing transition, the T_c and the clearing entropy, $\Delta S_{NI}/R$ with increasing methylene spacer length is indicative of the increased degree of conformation accessible to the spacer.[13]

The larger value of ΔS_{SN} /R shown by each of the respective azoLCPs correlates with the McMillan theory.[22] McMillan forecasts that the intensity of the smectic *A*-nematic mesophase transition is larger when the nematic temperature range gets smaller as indicated by the transitional entropy.[23] In addition, the enthalpy of the resultant transitions show an increasing trend with increasing methylene spacer length as observed previously for SCLCPs with azobenzene mesogens with a methoxy tail group.[24] This trend is ascribed to the decoupling of the mesogens from the polymer backbone as the spacer length increases due to its increasing flexibility.[20]

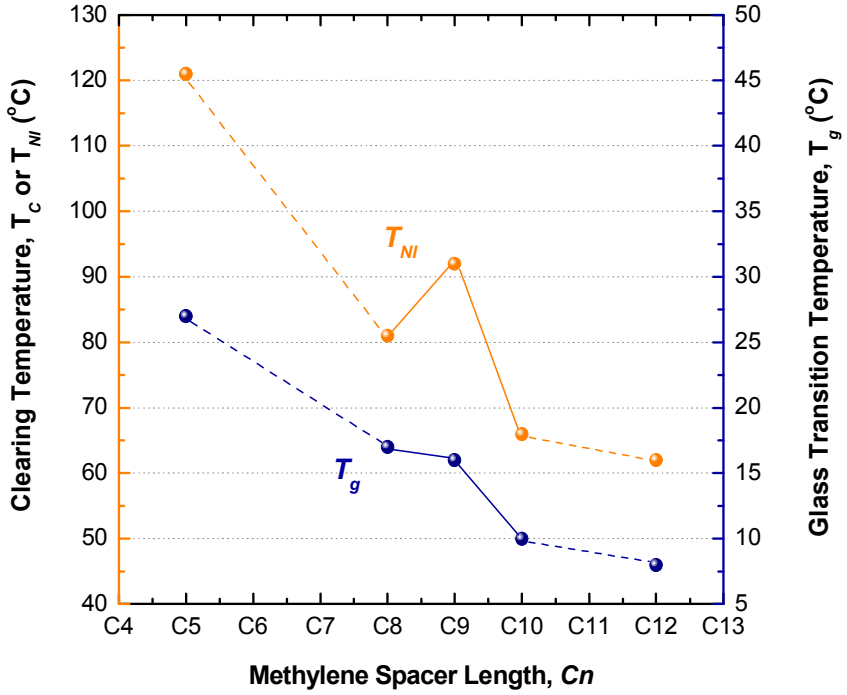

Fig. 5 Clearing, T_c and glass transition, T_g temperatures as a function of varying spacer length, *n* for the series of poly[4-(4'-cyanophenylazo)phenoxy]alky methacrylate polymers synthesized (azoLCP-C_5, azoLCP-C_8, azoLCP-C_9, azoLCP$_{10}$ and azoLCP-C_{12}).

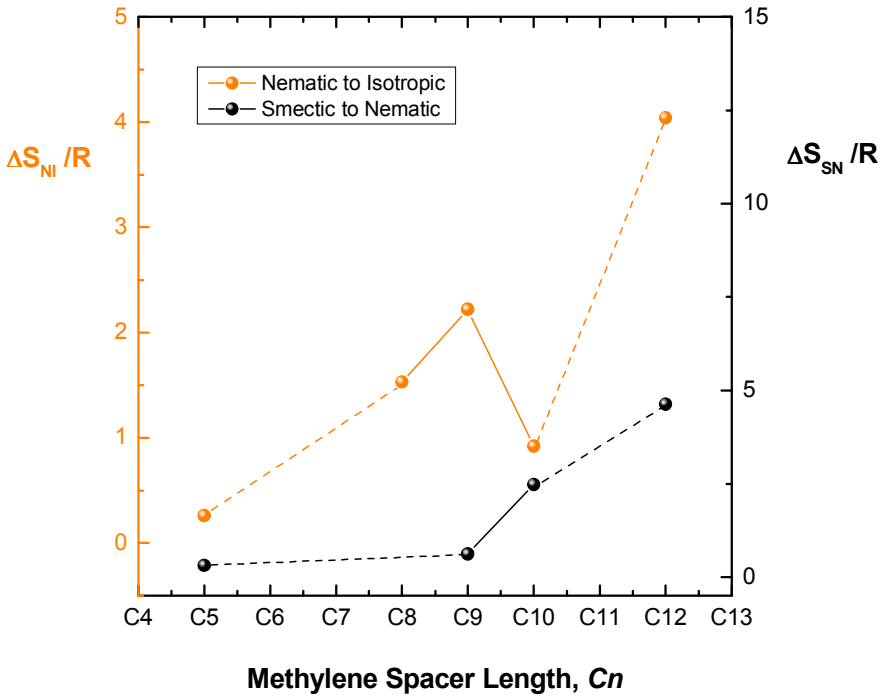

Fig. 6 Dependence of the entropy associated with the smectic-nematic ($\Delta S_{SN}/R$) and nematic-isotropic (clearing) ($\Delta S_{NI}/R$) transitions as a function of varying spacer length, *n* for the series of poly[4-(4'-cyanophenylazo)phenoxy]alky methacrylate polymers synthesized (azoLCP-C_5, azoLCP-C_8, azoLCP-C_9, azoLCP$_{10}$ and azoLCP-C_{12}).

Mesomorphic Phase Behavior by Polarizing Optical Microscopy

The azoLCPs were dissolved in THF and drop-cast onto micro-slides and air-dried to form films of non-uniform thicknesses. These films were then annealed by heating to temperatures above the T_g but ~10 ^oC below the T_c of each specific azoLCP-C$_n$. Under POM, all polymers in the azoLCP-C$_n$ series showed birefringence. Distinct focal conic fan textures were observed for all azoLCPs at room temperature (22 ^oC). These textures were assigned to the smectic *A* mesophase.[25]

Heating above the temperature connected with the lower temperature endotherm in the initial heating DSC scan for each azoLCP produces *schlieren* textures indicative of a nematic phase.[26] This phase persists until the higher temperature endotherm in the second heating DSC scan linked to the clearing transition or isotropic state, is reached and exceeded. Representative images obtained from POM for azoLCP-C$_9$ is shown in **Fig. 7**. The nematic and smectic *A* mesophases observed in the POM occurs at temperatures that correlated well with the T_{NI} and T_{SN}, obtained from the DSC scans for the respective azoLCPs. And, as discussed in the next section, the identities of these phases have been corroborated with X-ray diffraction experiments.

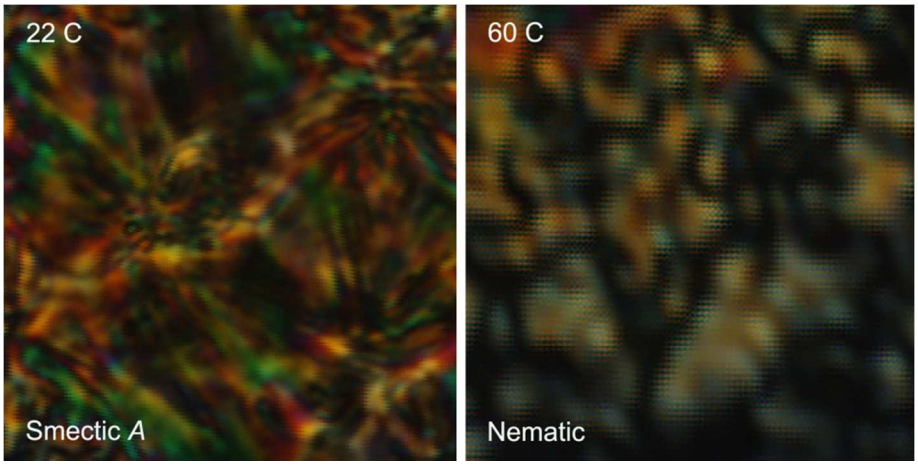

Fig. 7 Polarizing optical micrographs of smectic *A* focal conic fan texture (22 ^{o}C) and nematic *schlieren* texture (60 ^{o}C) exhibited by azoLCP-C_9. Magnification x100.

Mesogen Orientation in SCLCP by Wide Angle X-ray Diffraction Analysis

WAXD analysis was employed to study the azoLCPs' lattice structure. The diffraction patterns are shown in **Fig. 8a** and confirm a high degree of crystallinity in each film, annealed for 30 min above its respective T_g. Closer examination of the X-ray diffraction patterns reveals the structural effects of spacer length, l_{spacer} on these SCLCPs. The distance between the crystal planes is calculated as *d*-spacing indicated by Bragg's law[27] according to **Equation 1**, where *n* is the order of scattered reflection, λ is the wavelength of incident X-rays (for Cu-kα, λ = 1.54 Å), and θ is the scattering angle.

$$n\lambda = 2d\sin\theta \qquad [1]$$

The Scherrer's relationship[28] shown in **Equation 2** is used to calculate the crystallite size, τ of the scattering domain. *K* is the shape factor which is assumed as 0.9 for most polymers.[29] β

is known as the full-width-at-half-maximum of the crystalline peak. The value of β is expressed in radians for purposes of these calculations.

$$\tau = \frac{K\lambda}{\beta \cos\theta} \qquad [2]$$

As shown in **Fig. 8a** the first-order peaks form between ~1.5° and ~3°, corresponding to a lamellar spacing ~57 to 30 Å according to Bragg's Law. Based on comparison with other research on LCP polymers, this lamellar feature is attributed to the interchain layer size, rather than the distance between mesogens. The π-stacking interaction that dominates mesogen spacing is expected to be on the order of 2-4 μm, which was not observed, but would appear around 20-40 degrees on the X-ray pattern. Calculated interchain-spacing, d_1 and crystalline domain size, τ for each azoLCP are tabulated in **Table 3**. The peaks do not grow appreciably above baseline, but they shift to slightly higher angles after an extended anneal, indicating tightening of the crystal structure.

In **Fig. 8b** the WAXD spectra of the azoLCP films are shown, after heating each polymer above its respective T_c followed by quench-cooling the films in liquid N_2 to preserve the isotropic or "*melt*" phase. Once the films were heated above their respective isotropic temperatures ("*melted*") and rapidly quenched-cooled using liquid nitrogen, crystallinity was lost and the polymer film was preserved in an isotropic state. Quenching helps to freeze the LC mesogens in an isotropic phase even after the azoLCPs samples are equilibrated to room temperature (22 ^{o}C), though in theory, the azoLCPs with T_g below room temperature could begin to crystallize if given enough time. Indeed, the "*melt-quench*" sequence appears to remove the lamellar peaks, indicating that the isotropic phase is recovered.

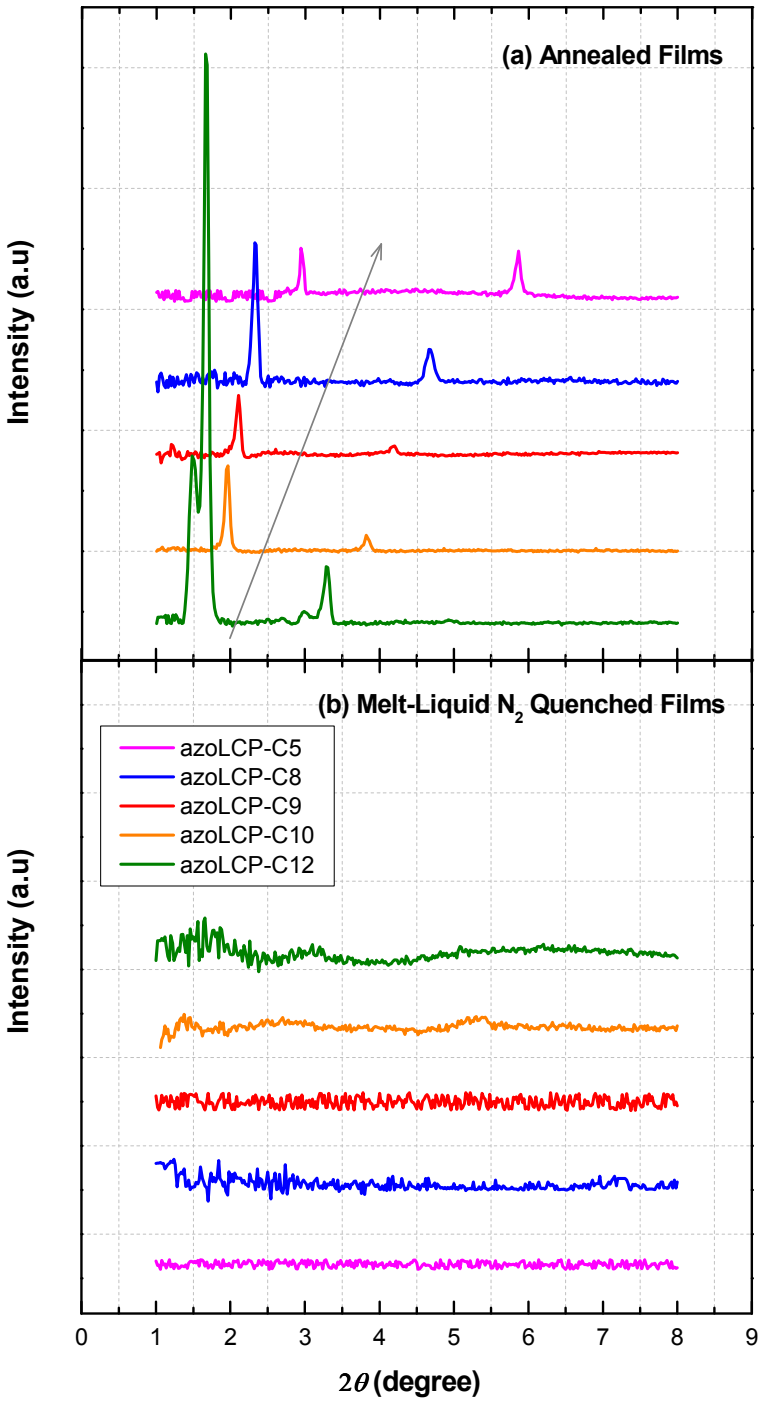

Fig. 8 WAXD data for poly[4-(4'-cyanophenylazo)phenoxy]alky methacrylate polymers (azoLCP-C_5, azoLCP-C_8, azoLCP-C_9, azoLCP-C_{10} and azoLCP-C_{12}) showing (a) the annealed polymer film which gives the liquid crystalline peaks corresponding to the smectic phase, and (b) after heating the polymer films above their respective clearing temperatures followed by rapid quench-cooling the films in liquid N_2 to preserve the isotropic or "*melt*" phase. The arrow indicates decreasing methylene spacer length.

Table 3 Crystal Lattice Spacing and Crystalline Domain Size of azoLCPs as a Function of Methylene Spacer Length

AzoLCP (spacer)	Peak angles (^{o})	d_1 at θ_1 (nm)	d_2 at θ_2 (nm)	Crystalline grain size τ (nm)
azoLCP-C_5	2.90	30.42	-	79.68
azoLCP-C_8	2.35	37.42	-	79.67
azoLCP-C_9	2.10	42.07	-	79.67
azoLCP-C_{10}	1.88	46.95	-	79.68
azoLCP-C_{12}	**1.55, 1.70	**56.92	51.90	79.66

The crystal domain size, τ (or persistence of lamellar order) does not vary with mesogen spacer length. This is not unexpected because the crystal persistence is related to the nucleation density upon crystallization, which depends on the crystallization protocol. All samples were annealed at the same temperature above their T_g, thus similar crystallite sizes are expected. The backbone arrangement suggests a smectic phase, whereas the mesogen spacing would occur at much higher angle as mentioned previously.[10] The wide-angle peak associated with mesogen spacing is not observed in our azoLCPs likely due to limited instrument sensitivity.

Upon close observation, a split peak can be seen in the scattering pattern of the azoLCP-C_{12} at 1.55° and 1.70°. This is indicative of two populations of backbone crystal that correspond to local energetic minima at two possible levels of interdigitation, also sometimes known as two-layer packing of LC backbones.[2] On the basis of this observation a schematic of the two possible levels of interdigitation of the mesogens is shown in **Fig. 9**. As reported previously,[10] smectic

periods for small molecules correspond to mesogen length, $l_{mesogen}$ but the constraint of the polymer backbone and the presence of the cyano-end groups present an environment where significant deviance from this spacing is possible. Given that the azobenzene mesogen is likely ~1.23 nm long, it is clear that the mesogens are not completely interdigitated. As previously reported for azobenzene containing SCLPs albeit with a nitro-substituent as a tail-group,[21,30] the spacer length grows with smectic layer spacing as shown in **Fig. 9**.

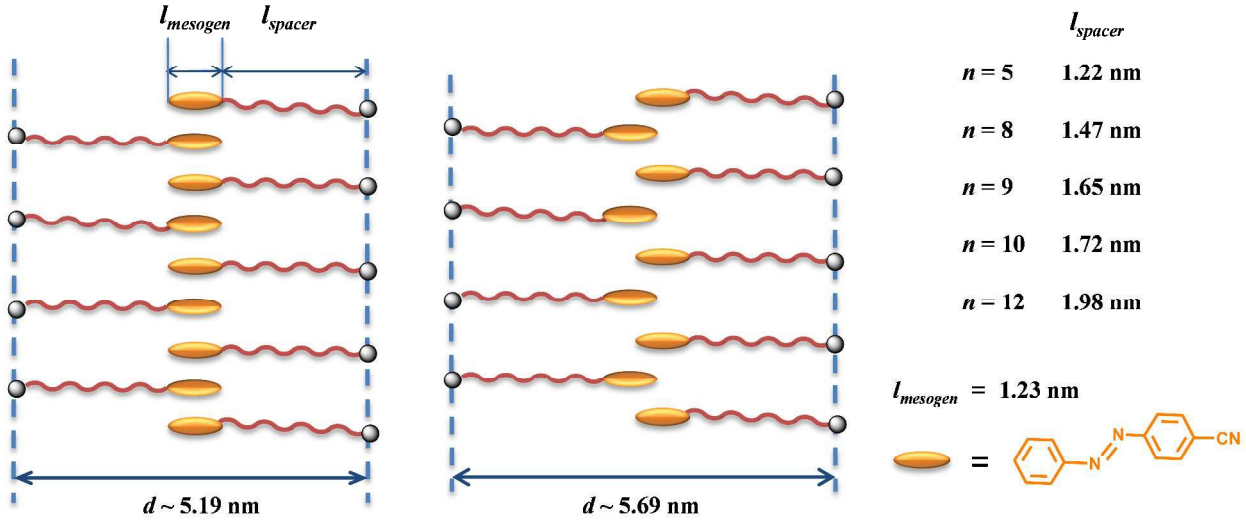

Fig. 9 Schematic illustrating two different populations of polymer backbones that correspond to local energetic minima at two different levels of interdigitation as observed in the WAXD of azoLCP-C_{12} polymer. Note schematic is not drawn to scale and is for illustrative purposes only.

Based on the crystal morphology analysis, it is anticipated that permeability should be relatively independent of spacer length, because no significant differences in equilibrium crystallinity or crystal perfection are detected. Furthermore, the grain size appears similar for all polymers leaving similar "*porous*" amorphous regions around the crystalline regions for gas to permeate. However, as the thermal analysis suggests, the spacer length selection allows tuning of

the switching temperature. In the "*open*" state, however, the permeability could depend on the flexibility of the particular polymer at the measurement temperature.

Oxygen Permeation Analysis

The oxygen permeation analyzer (OPA) instrument does not have heating capability, and so in order to make permeability measurements on films above their T_c or T_{NI}, where the azoLCP will be in an isotropic phase, the films were first heated above T_c, held for 30 min for thermal equilibrium to be reached followed by rapid quenching in liquid N_2 (*melt-liquid N_2 quenched*) in order to "*freeze-in*" the isotropic phase. The assumption is made that the measurement time is less than the time taken for the film to return to room temperature where it will be in a crystalline mesomorphic phase (nematic).

The amount of permeant detected by the instrument is proportional to the amount of molecules that permeate through the polymer films and is quantified as oxygen permeance or oxygen transmission rate (OTR). Reduced permeability for the polymer films after annealing is observed in every azoLCP homologue of the series as shown in **Table 4**. In fact, the OTR of the "*melt-liquid N_2 quenched*" films is 10-times larger than that of the annealed films. These results demonstrate that annealing the films results in a decrease in P_{O_2} of this film, while heating above its T_c increase its permeability. The phenomenon that liquid crystalline order is induced by annealing while liquid crystalline order vanished by heating above T_c and subsequent cooling with liquid N_2 was also confirmed by WAXD and POM, as discussed in the previous sections.

Switching of gas permeability is accomplished by heating which corresponds to switching from a highly crystalline smectic phase to an amorphous isotropic phase, in other-words a "*closed*" to "*open*" lattice spacing. This order of magnitude difference in the permeability of films from "*closed*" to "*open*" mesophases is illustrated schematically in **Fig. 10**.

Table 4 Oxygen permeance (OTR) and permeability (P_{O_2}) coefficients for the azoLCPs in "*closed*" and "*open*" states that correspond to annealed and "*melt-liquid N_2 quenched*" conditions, respectively

AzoLCP (spacer)	**Polymer Film Conditions**	**O_2 Permeance (OTR) ($cm^3/(m^2.day.atm)$)**	**O_2 Permeability (P_{O_2}) Coefficient (1×10^{13}) ($cm^3.cm/(m^2.s.Pa)$)**
azoLCP-C_5	Annealed at 85 °C	1,056	0.013
	Melt-quenched	76,579	0.493
azoLCP-C_8	Annealed at 65 °C	964	0.012
	Melt-quenched	32,400	0.406
azoLCP-C_9	Annealed at 65 °C	2,153	0.027
	Melt-quenched	24,717	0.310
azoLCP-C_{10}	Annealed at 65 °C	1,992	0.024
	Melt-quenched	33,559	0.402
azoLCP-C_{12}	Annealed at 65 °C	1,483	0.019
	Melt-quenched	22,055	0.277
PEMA	25 °C	-	0.863[31]
HDPE		-	0.302[32]
LDPE		-	2.160[32]
PMMA		-	0.116[33]

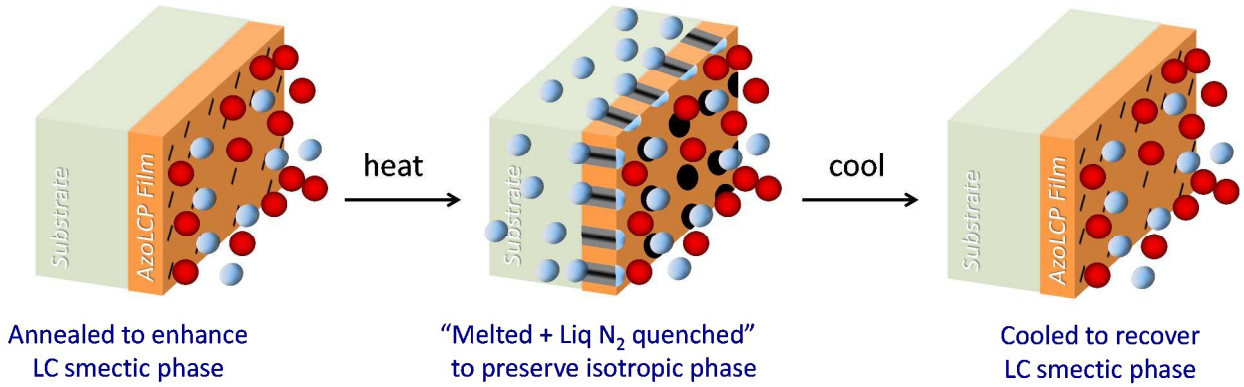

Fig. 10 Depiction of phase-switching upon heating in liquid crystalline polymer films. Films are annealed to "*close*" and then heated to above the isotropic temperature to "*melt*" followed by quench cooling using liquid N_2 to "*open*" the lattice spacing.

It is important to note that the permeability results are slightly higher than expected for azoLCP-C_{10}. A plausible explanation for this is as follows: as annealed films start to orient themselves in the liquid crystalline order, they exist in nematic or smectic phases at a given temperature. But for some of these polymers, smectic or nematic liquid crystalline states may co-exist due to the difference in their kinetics of crystallization at any given enthalpic condition, which results in different permeability readings in the annealed state. Since these experiments are performed in a closed cell which is kept at the room temperature, controlling the crystallization kinetics is not trivial. Indeed, the first heating cycle of the DSC data (ESI **Fig. S8-12†**) provided evidence of this co-existence of liquid crystalline phases and is a plausible explanation why asymmetry in the permeability is observed in the "*closed*" state or annealed state.

These P_{O_2} results for the azoLCPs in the "*closed*" state or smectic-nematic liquid crystaline phase at temperatures below the T_c is more similar to that found for side-chain liquid-crystalline polyacrylates containing 4-cyanophenyl 4-hexyloxybenzoate-based mesogenic side groups[34] at 1.11 x 10^{13} cm^3.cm/ (cm^3.s.Pa) at 25 ^oC (nematic liquid crystalline phase), than they are for P_{O_2} measurements made by Lui *et al*.[4] Indeed for poly(5-[4'-cyanophenylazo)phenoxy]propylmethacrylate) with (5) methylene spacer groups the current work found the OTR to be 1,056 $cm^3/(m^2$.day.atm) for annealed films compared to 1.56 x 10^{-3} $cm^3/(m^2$.day.atm) found by Lui *et al*.[4] Non-discrimination of the reaction with O_2 or water is assumed to be the reason for the relatively low OTR measurements in the latter case. Also seen in **Table 4**, the P_{O_2} results for the azoLCPs in the "*open*" state are only slightly higher than that of high-density polyethylene,[32] HDPE and lower than those of low-density polyethylene,[32] LDPE, poly(ethyl methacrylate) PEMA,[31] and PMMA,[33] respectively at 25 ^oC.

Conclusions

We successfully synthesized a series of azobenzene containing side chain liquid crystalline polymers (azoLCPs) with different flexible spacer group lengths (C_5, C_8, C_9, C_{10}, C_{12}) and characterized the relationship between their switchable O_2 gas permeability properties and LC mesophase structures. Switching of O_2 gas permeability is accomplished by heating which corresponds to highly crystalline nematic phase to a less crystalline isotropic phase, in other-words a "*closed*" to "*open*" lattice spacing. Increasing the methylene spacer length had little or no effect on O_2 gas permeability properties however it did decrease the T_c, allowing fine control of the temperature at which the switch in O_2 gas permeability properties takes place by tuning the

mesophase between nematic and isotropic states. Such an ability to tune O_2 gas permeability properties of the azoLCP-C_n film by an order of magnitude can have potential applications in "*smart*" textiles. It is envisioned that thermally responsive azoLCP films can be applied to textiles to achieve "*smart*" textile functionality, whereby the gas vapor permeability increases at higher temperatures (to promote cooling) and decreases at lower temperatures (to trap warm air) thereby protecting the wearer from dramatic temperature changes in the environment.

Acknowledgements

Dr. Dan Schmidt is gratefully acknowledged for assistance with the WAXD and OPA experiments. S.H. acknowledges Soujanya Muralidhara and Bin Tan for assistance with the GPC set-up, molecular weight analyses and WAXD analyses, respectively.

References

1 C.B. McArdle, *Scope and Potential of Polymeric systems with side chains*, 1989.

2 L. H. Sperling, in *Introduction to Physical Polymer Science*, John Wiley & Sons, Inc., 2005, pp. 325–348.

3 T. Ikeda, J. Mamiya and Y. Yu, *Angew. Chem. Int. Ed.*, 2007, **46**, 506–528.

4 J. Liu, M. Wang, M. Dong, L. Gao and J. Tian, *Macromol. Rapid Commun.*, 2011, **32**, 1557–1562.

5 E. Glowacki, K. L. Marshall and C. W. Tang, ed. I. C. Khoo, 2009, p. 74140H–74140H–13.

6 K. G. Gutiérrez-Cuevas, L. Larios-López, R. J. Rodríguez-González, B. Donnio and D. Navarro-Rodríguez, *Liq. Cryst.*, 2013, **40**, 534–545.

7 A. A. Craig and C. T. Imrie, *Macromolecules*, 1995, **28**, 3617–3624.

8 Y.-S. Xu, D. Shi, J. Gu, Z. Lei, H.-L. Xie, T.-P. Zhao, S. Yang and E.-Q. Chen, *Polym. Chem.*, 2016, **7**, 462–473.

9 C. He, C. Zhang and O. Zhang, *Polym. Int.*, 2009, **58**, 1071–1077.

10 P. Davidson, *Prog. Polym. Sci.*, 1996, **21**, 893–950.

11 E. Głowacki, K. Horovitz, C. W. Tang and K. L. Marshall, *Adv. Funct. Mater.*, 2010, **20**, 2778–2785.

12 T. KAJIYAMA, *Chem. Lett.*, 1979, S, pp. 679–682,.

13 A. A. Craig, I. Winchester, P. C. Madden, P. Larcey, I. W. Hamley and C. T. Imrie, *Polymer*, 1998, **39**, 1197–1205.

14 D. Wang and X. Wang, *Top. Issue Polym. Self-Assem.*, 2013, **38**, 271–301.

15 D. Wang, J. Liu, G. Ye and X. Wang, *Polymer*, 2009, **50**, 418–427.

16 A. Natansohn, P. Rochon, J. Gosselin and S. Xie, *Macromolecules*, 1992, **25**, 2268–2273.

17 L. Ding and T. P. Russell, *Macromolecules*, 2007, **40**, 2267–2270.

18 T. Kashiwagi, A. Inaba, J. E. Brown, K. Hatada, T. Kitayama and E. Masuda, *Macromolecules*, 1986, **19**, 2160–2168.

19 X.-Q. Zhu, J.-H. Liu, Y.-X. Liu and E.-Q. Chen, *Polymer*, 2008, **49**, 3103–3110.

20 C. Pugh and A. L. Kiste, *Liq. Cryst. Polym. Part 3*, 1997, **22**, 601–691.

21 S. Freiberg, F. Lagugné-Labarthet, P. Rochon and A. Natansohn, *Macromolecules*, 2003, **36**, 2680–2688.

22 W. L. McMillan, *Phys. Rev. A*, 1971, **4**, 1238–1246.

23 R. W. Date, C. T. Imrie, G. R. Luckhurst and J. M. Seddon, *Liq. Cryst.*, 1992, **12**, 203–238.

24 T. Hu, J. Yi, J. Xiao and H. Zhang, *Polym J*, 2010, **42**, 752–758.

25 I. Dierking, in *Textures of Liquid Crystals*, Wiley-VCH Verlag GmbH & Co. KGaA, 2003, pp. 91–122.

26 I. Dierking, in *Textures of Liquid Crystals*, Wiley-VCH Verlag GmbH & Co. KGaA, 2003, pp. 51–74.

27 W. H. Bragg and W. L. Bragg, *Proc. R. Soc. Lond. Math. Phys. Eng. Sci.*, 1913, **88**, 428–438.

28 A. L. Patterson, *Phys. Rev.*, 1939, **56**, 978–982.

29 R. Jenkins and R. L. Snyder, in *Introduction to X-ray Powder Diffractometry*, John Wiley & Sons, Inc., 1996, pp. 47–95.

30 M. Kamruzzaman, Y. Kuwahara, T. Ogata, S. Ujiie and S. Kurihara, *J. Appl. Polym. Sci.*, 2011, **120**, 950–959.

31 V. Stannett and J. L. Williams, *J. Polym. Sci. Part C Polym. Symp.*, 1965, **10**, 45–59.

32 A. S. Michaels and H. J. Bixler, *J. Polym. Sci.*, 1961, **50**, 413–439.

33 W.-H. Yang, V. F. Smolen and N. A. Peppas, *J. Membr. Sci.*, 1981, **9**, 53–67.

34 D.-S. Chen, G.-H. Hsiue and C.-S. Hsu, *Makromol. Chem.*, 1992, **193**, 1469–1479.

Table of Content Graphic

Title: Tuning Oxygen Permeability in Azobenzene-Containing Side-Chain Liquid Crystalline Polymers

Author(s), and Corresponding Authors:

*Syed Hassan, Robinson Anandakathir, Margaret J. Sobkowicz and Bridgette M. Budhlall**

Department of Plastics Engineering and NSF Center for High-Rate Nanomanufacturing,

University of Massachusetts, Lowell, MA. 01854.

*Corresponding author email: Bridgette_Budhlall@uml.edu

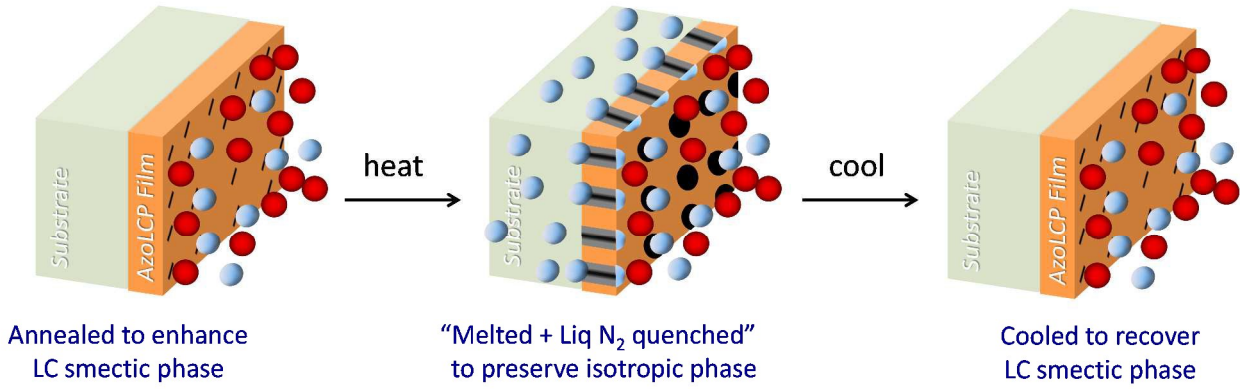

Tuning oxygen permeability in azobenzene-containing side-chain liquid crystalline polymers was achieved by control of their mesomorphoric phases.